IJBEM
Vol. 7, No. 2, 2005

Wavefront-based inverse electrocardiography using an evolving curve state vector and phenomenological propagation and potential models

Alireza Ghodrati[1], Dana H. Brooks[1], Gilead Tadmor[1], Bonnie Punske[2], and Rob MacLeod[2]
[1]Department of Electrical and Computer Engineering, Northeastern University, Boston, MA, USA
[2]Nora Eccles Harrison Cardiovascular Research and Training Institute (CVRTI), University of Utah, Salt Lake City, Utah, USA

Abstract— **We report on an initial study of a state-space model for propagation of the activation wavefront on the heart surface. The activation wavefront was modeled as a curve evolving on the heart surface with the evolution governed by factors derived from *a priori* data, including anisotropy, along with study of epicardial measurements. The body-surface potential / wavefront relationship is modeled via an intermediate mapping of wavefront to epicardial potentials, again derived from data and prior physiological factors. This design avoids the over-smoothing of Tikhonov solutions and is capable of flexible inclusion of physiological information, including fiber orientation, in the model. Initial results show improvements in reconstructing activation wavefront with respect to the Tikhonov solution, especially at early activation times.**

I. Introduction

Recent work on inverse solutions for electrocardiography have generally used either an activation wavefront-based model or a potential-based model (using epicardial, endocardial, or trans-membrane potentials)[1], [2], [3], [4]. Activation-based models reduce the unknowns to the arrival time of the wavefront at each point on the epicardial and endocardial surfaces while potential-based models treat the value of the potential at each point on the relevant surface at each time instant as a free variable.

Activation-based models are low order parameterizations which capture the single most important physiological feature of cardiac propagation but depend on isotropy / homogeneity assumptions and a fixed shape of the temporal waveforms in order to form a tractable forward model. Potential-based models are less restrictive but imply a high-order parameterization. Thus they are not robust without considerable smoothing (regularization), and make it difficult to include the physical and geometric constraints imposed by the central physiological feature, namely wavefront behavior, except via indirect and somewhat coarse models [1], [4].

So activation-based methods are generally more robust than potential models, for instance to error in geometry or noise in measurements [5], but they may not take advantage of information about the cardiac sources potentially present in the measurements and they cannot take advantage of known prior information about non-isotropic propagation of wavefronts and true 3D nature of propagation. Our goal here is to propose a model which can relax isotropy and homogeneity assumptions, and include prior physiology and electrophysiology, while maintaining the low dimensionality implied by wavefront behavior. As a first step, we propose a model which has the following characteristics:

1) The quantity of interest is the location of the wavefront on the epicardial surface at each instant in time. The wavefront is modelled as a continuous 1D curve on that (2D) surface, using a discrete representation for computational purposes.
2) The wavefront evolves in time by propagating in the direction normal to the curve according to a possibly time- and space-varying velocity function.
3) The potentials on the heart surface, as in activation models, are completely determined (at least in the current model) by the wavefront location at each time. However we are free to choose time- and space-varying mechanistic models for this relationship.
4) The body surface potentials are determined by a standard potential-to-potential forward model.
5) The parameters that determine the time- and space-varying velocity function and the time- and space-varying wavefront-to-potential function will be chosen through a phenomenological approach, via study of measured data and fitting of appropriate parameters.

Thus we need three equations to describe this formulation: one which describes how the wavefront curve evolves from one time instant to another, one which maps the wavefront location at any particular time to the epicardial potentials, and thirdly the standard potential-based forward model which maps epicardial to body-surface potentials.

Viewing this formulation from the perspective of the inverse problem, then the goal is to use the data—body surface measurements—to determine the location for the wavefront curve at each point in time. Thus the wavefront curve represents the true unknown *state* of the system: if we know it at a given time instant, and we have the parameters of the two mapping functions, we have a model for the measurements. Thus this formulation is a natural fit to a non-linear state-space model, which we propose to solve using an Extended Kalman Filter (EKF) [6] approach.

As an initial step, we concentrate in what follows on beats that are initiated by a stimulus on the epicardium. Due to the relative geometric and physiological simplicity of the ensuing propagation, this is the simplest case for this model.

II. METHODS

A. State-space framework

The basis of our proposed model is the idea that the wavefront, conceived of as a curve on the epicardial surface at each time instant, is sufficient, along with a model, to determine the potentials on the the body surface at that time instant, to within a reasonable level of uncertainty. Thus we treat the wavefront as the state of the system, and this enables an appropriate state-space formulation. We model this state as a continuous curve in an infinite-dimensional space, although we treat it computationally at a given time instant via a discrete finite-dimensional representation. This leads to a nonlinear state evolution function and a nonlinear forward model (since the forward model includes the mapping from wavefront to epicardial potentials as well as from epicardial potentials to body surface potentials). The result is the following pair of equations:

$$\begin{cases} c_{n+1} = f(c_n) + u_{n+1} \\ y_{n+1} = Ag(c_{n+1}) + w_{n+1} \end{cases} \quad (1)$$

where subscript n represents the time instant, c is the curve representing the wavefront, y is an $M \times 1$ vector holding torso potentials, A is an $M \times N$ matrix representing the forward model, f is the state evolution function, g is a function that returns the epicardial potentials from the activation wavefront and u and w are Gaussian white noise variables that represent the temporal model error and forward problem error respectively : $w_n \sim N(0, C_n)$, $u_n \sim N(0, Q_n)$.

Finding appropriate functions f and g is the most crucial part of building the model, as we describe in the next two sections.

B. State evolution function

This function models the propagation of the activation wavefront in time. The input to the function is the wavefront curve at the current time instant and the output is the wavefront curve at the next time instant. The model should reflect to the extent reasonable the behavior of the three dimensional myocardium.

To evolve the curve on the heart surface we need to know the speed in the normal direction at each point of the curve at each time instant. Based on our own studies of a number of canine beats provided by our collaborators at CVRTI, and in accordance with the observations reported in [7], [8], we note the following rules for the wavefront speed :

1) The fiber direction dominates other factors in the early activation time proportional to the projection of that direction onto the normal direction to the curve.
2) The speed increases with time after initiation and becomes essentially isotropic.
3) Certain locations on the epicardium tend to show higher (apex, right ventricle) or lower (over the septum) speeds, although there is some interaction of this effect with velocity direction.

Based on the these properties we modeled the speed as follows:

$$\upsilon(s,t) = \beta(t)\delta(s)(a(t)cos^2(\eta) + b(t)) \quad (2)$$

where $\upsilon(s,t)$ is the speed of a point at location s on the activation wavefront at time t after initiation, $\beta(t)$ models temporal factors and increases with time, $\delta(s)$ models spatial factors, η is the angle between the normal direction to the wavefront and the local fiber direction at s, and a and b are coefficients of the fiber direction effect. Hence the speed at time t along and across the fibers is proportional to $a(t)+b(t)$ and $b(t)$ respectively.

C. The model to determine epicardial potential from wavefront location

Our basic model of the potential surface is that it is divided into three regions: activated, inactive and transition. This model depends on removing the increasing trend in the reference documented in [9], which we estimate here by using late-activated regions for early time instants and early-activated regions for late time instants. After removing the reference, the potential of the activated region at each time instant is taken as having a constant, and negative, value while the potential of the inactive region is treated as being zero. The transition region between activated and inactive regions has a more complicated behavior. To represent this effect we assume that the potential at each point on the heart surface is a function of the distance from that point to the wavefront curve. Note that this function describes a profile of the potential surface in the direction normal to the wavefront. We modeled this function with the step response of a second order system:

$$\begin{cases} \Gamma(d) = \alpha\frac{V}{2}(1 - \frac{1}{\sqrt{1-\xi^2}}e^{-\xi\omega d}\sin(\omega\sqrt{1-\xi^2}d + \psi)) \\ \qquad\qquad -\frac{V}{2} + \mathrm{ref} \end{cases} \quad (3)$$

where $\psi = \arctan(\frac{\sqrt{1-\xi^2}}{\xi})$, Γ is the potential function at any point on the heart surface, d is the distance of that point to the wavefront curve, α is -1 for points inside the wavefront curve and 1 for points outside the curve, V is the negative potential value of the activated region, ω and ξ control the slope and overshoot of the potential function, respectively, and ref represents the reference potential.

Fig. 1 shows Γ as a function of the distance d for different values of ω and ξ for $V = 20mV$ and $\alpha = 1$ which means the point is outside the wavefront curve. The potential far from the wavefront curve is constant with value either zero (outside the curve) or $-V$ (inside the curve). Thus the specific values of ω and ξ are important just in the transition region, and Γ gives us flexibility to have different slopes and magnitude of overshoot or undershoot in different locations.

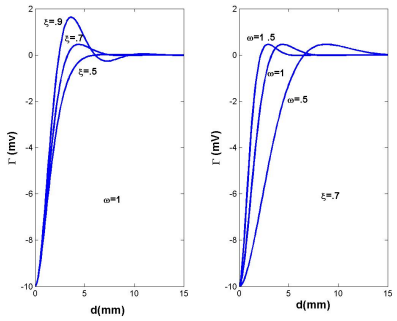

Fig. 1. Function Γ versus distance d for different values of ξ and ω

Our studies of canine epicardial data showed a weak correlation between the parameters of Γ and both fiber directions and increasing time. Using parameters fit to these studies we predefine Γ as a function of distance, fiber directions and time. (We note that we can achieve increased flexibility if we include parameters of Γ in the state variable and estimate them using the body surface measurements.

D. Filtering of the residual

The estimate of the state-space model at each time instant in the EKF algorithm is a combination of the prediction obtained from the previous solution and a correction term which depends on the current measurements via minimization of the residual norm $||y_n - Ag(c_n)||$. Since our model assumes that the potentials in the activated and inactivated regions are constant we expect to have a systematic error component in the model which will effect the predicted body surface measurements $Ag(c_n)$. Moreover, the transition region has a much more complicated behavior than our model allows. We observed that this error effects the residual norm even if we use the *true* wavefront location. Thus the danger is that minimizing the residual under these circumstances, after a certain point, will fit the error in the model rather than the wavefront location itself.

However the major effect of this epicardial potential surface model error on the body surface potentials was low frequency, and indeed was well matched to the low-order left singular vectors of the forward matrix A. Thus we attenuated its effect on the residual norm by minimizing the filtered residual, multiplying by the transpose of U_k, where U_k contains columns $k+1$ to N of U, the left singular matrix of A, $A = U\Sigma V^T$:

$$U_k^T(y_n - Ag(c_n)) \tag{4}$$

This filtering removes information in the residual which could be important in standard regularization and might even make such a problem singular. But it turns out not to be of great importance in our state-space model, presumably because of the strong constraints imposed by the temporal model and potential model. The order of the filtering, k, is an important factor which we found empirically from the data.

III. Results

We implemented a simple version of the model and tested it using canine data from tank experiments conducted by our collaborators at CVRTI [10]. The data to which we fit the model parameters described in the previous sections included multiple beats from multiple animals, so that it was not overly tailored to the test beat used in the simulation reported here.

From the epicardial potentials we simulated the potentials on the torso surface using a linear forward model based on a Boundary Element Method solution for the homogeneous tank geometry (the matrix A above) and added Gaussian white noise to achieve a 30dB signal to noise ratio. The dimensions of A were 771×490: 490 nodes in the heart geometry model mapped into 771 electrodes on the torso. Fiber directions were approximated from the Hunter heart[13].

We represented the wavefront curve in a spherical coordinate system using a limited number of points which we interpolated using B-spline basis functions. We allowed the number of points used to represent this curve to grow as the activated area got larger; since this was merely a representation of the continuous curve we avoided problems that would otherwise be caused by changing the dimension of the state-space. We did have to handle changing dimensions of the matrix representing the error covariance of the state variables, which we achieved through a simple interpolation scheme.

We used (2) and (3) to implement the functions f and g. The reference was estimated from the true data and used in (3). We obtained the parameters of the functions f and g from beats with pacing sites on both the left and right ventricles. We approximated the speed of the wavefront at each point on the heart surface by calculating the time required for the wavefront to travel a fixed distance in the neighborhood of that point. For simplicity in this initial implementation we set $a(t) = .6$, $b(t) = .3$, $\beta = 1$ and $\delta = 1$ in (2). To determine the potential model we approximated the spatial gradient of the potential along the normal direction to the wavefront at different points on the wavefront and at different time instants. The resulting parameter values were $\omega = .7$ and $\xi = .7cos^2(\eta) + .5$. We used the EKF algorithm to solve the state-space model, linearizing the functions f and g by using a finite difference method.

Fig. 2 shows the wavefront obtained from the true solution (Red) along with the reconstructed wavefront using our method (white) and the wavefront obtained from the Tikhonov solution. In all cases the wavefront was defined as the set of points whose potential equaled the average of the activated and inactive potential values. As can be seen in the figure, the proposed method was more accurate,

especially for early activation time when the activated region was stretched along the local fiber directions.

IV. Conclusion

We used a state-space formulation to solve the inverse problem of ECG. The basic motivation was to add physiological information about cardiac propagation to a low-dimensional, wavefront-based model. This information appears in the state evolution function of our state-space model. The use of the wavefront curve as the state variable (in contrast with earlier Kalman filtering approaches for inverse electrocardiography which used the potentials as the state variable [11], [12]) both enforced the sharp transition across the wavefront and provided a low-dimensional, and therefore potentially more robust, model. Moreover the structure of the model facilitates our ability to include physiological properties of the heart such as fiber orientation.

To create the state evolution model we needed the speed of the wavefront in the normal direction, which we modeled as a function of local fiber orientation. We applied fixed model to calculate epicardial potentials from the wavefront. We used an EKF approach to solve the state-space system and reconstructed the activation wavefront. Results showed improvement with respect to the Tikhonov solution especially at early activation times.

The results here are just a first step in building an appropriate model. We only used the fiber directions of the heart surface for our propagation model while a more complete model should consider the three dimensional effect of the fibers in the heart volume. We anticipate improvement by fixing $\beta(t)$ and $\delta(t)$ to reflect known behaviors. Moreover we intend to experiment with a potentially more accurate approach to model the potential surface by including the parameters of the potential model in the state variable. One goal of interest would be to estimate the positive regions which precede the wavefront in early activation and whose behavior reflects, among other factors, the depth of the pacing site in the myocardium. The reference potential that was used in our initial tests was obtained from the true solution. In the future we will need to estimate it from the torso measurements. Finally, a significant future challenge for this approach will be to model multiple wavefronts, breakthroughs, and disappearing wavefronts.

Acknowledgment

The authors are indebted to Bruno Taccardi for his advice, encouragement, and critical comments on our work. This work was supported in part by the National Institutes of Health, National Center for Research Resources, grant number 1-P41-RR12553-3.

References

[1] D.H. Brooks, G.F. Ahmad, R.S. MacLeod, and G.M. Maratos. *Inverse electrocardiography by simultaneous imposition of multiple constraints*, IEEE Trans. Biomed. Eng. vol. 46, pp. 3-18, 1999.

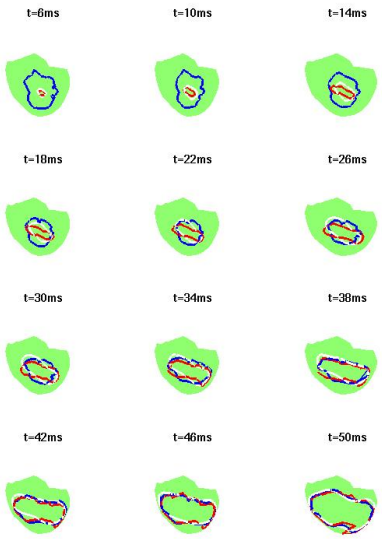

Fig. 2. Wavefront from true solution (Red), Tikhonov solution (blue) and our method (white), t shows the time with respect to the pacing

[2] G.J.M. Huiskamp and F.S. Greensite, *A new method for myocardial activation imaging*, IEEE Trans. Biomed. Eng., vol. 44, pp. 433-446, 1997.

[3] Pullan A.J., Cheng L.K., Nash M.P., Bradley C.P., Paterson D.J., *Non-invasive electrical imaging of the heart: theory and model development*, Annals of Biomedical Eng., 29(10):817-36, October 2001.

[4] Messnarz B, Tilg B, Modre R, Fischer G, Hanser F, *A new spatiotemporal regularization approach for reconstruction of cardiac transmembrane potential patterns*, IEEE Trans. Biomed. Eng., vol. 51, pp. 273-281, 2004.

[5] L. K. Cheng, J. M. Bodley, A. J. Pullan, *Effects of experimental and modeling errors on electrocardiographic inverse formulations*, IEEE Trans. Biomed. Eng., vol. 50, pp. 23-32, 2003.

[6] S. M. Kay, *Fundamentals Of Statistical Signal Processing: Estimation Theory*, chapter 12, pp. 391, Prentice Hall, New Jersey 1993.

[7] B Taccardi, E Macchi, RL Lux, PR Ershler, S Spaggiari, S Baruffi, Y Vyhmeister, *Effect of myocardial fiber direction on epicardial potentials*, Circulation, Dec 1994; 90: 3076 - 3090.

[8] B. Taccardi, R.L. Lux, P.R. Ershler, R.S. MacLeod, C. Zabawa, Y. Vyhmeister, *Potential distributions and excitation time maps recorded with high spatial resolution from the entire ventricular surface of exposed dog hearts*, Computers in Cardiology 1992. Proceedings. , 11-14 Oct. 1992, pp. 1-4.

[9] B. Taccardi, R.L. Lux, R.S. MacLeod, P.R. Ershler, T.J. Dustman, M. Scott, Y. Vyhmeister, N. Ingebrigtsen "Electrocardiographic waveforms and cardiac electric sources", J. Electrocardiol. 29 (Suppl.): 98-100, 1996.

[10] MacLeod R.S., Ni Q., Punske B., Ershler P.R., Yilmaz B., Taccardi B., *Effects of Heart Position on the Body-Surface ECG*, J. Electrocardiol., 33 Suppl: 229-237, 2000.

[11] J. El-Jakl, F. Champagnat, Y. Goussard, *Time-space regularization of the inverse problem of electrocardiography*, Proc. 17th Annu. Int. Conf. IEEE EMBS, 1995.

[12] Berrier KL, Sorensen DC , Khoury DS, *Solving the inverse problem of electrocardiography using a Duncan and Horn formulation of the Kalman filter*, IEEE Trans Biomed Eng vol. 51, pp. 507-515, 2004.

[13] Nielsen PM, Le Grice IJ, Smaill BH, Hunter PJ, *Mathematical model of geometry and fibrous structure of the heart*, American Journal of Physiology, 260, H1365H1378 (1991).